Smart Nanocarriers for Delivery of Anticancer Drugs: Recent Advances and Disadvantages

Nataliya Kutsevol and Antonina Naumenko

1 Introduction

Nowadays, chemotherapy is the major cancer treatment. However, low selectivity and wide side effect give additional problem to the clinical application of antitumor drugs. Chemotherapy damages both normal and tumor cells. Therefore, it is important to develop novel drug delivery systems for overcoming side effect and to improve the efficacy of anticancer drugs [1]. Nanotechnology is a promising approach for creation of highly efficient nanocarriers for modern cancer therapy, including dendrimers, polymeric nanoparticles, liposomes, etc. Polymer nanoparticles are considered as promising nanoplatform and nanocarrier for drug delivery [2]. Current reviews have demonstrated that polymer molecules have possibility to be accumulated by tumors [3]. However, most of water-soluble polymers cannot provide controllable drug release. To overcome this problem, stimuli-sensitive polymer as thermosensitive and pH-sensitive can be used for controlled release of drugs [4]. Such approach gives possibility to decrease the dosage of toxic drugs, although the drug concentration in tumor can be maintained for a much longer time [5].

Thus, such nanocarriers are considered as smart ones. However, for engineering of effective stimuli-responsive nanosystems, it should be deep knowledge on nanosystem biocompatibility and its capacity to load of antitumor drugs, stability, and toxicity of nanosystems. In this work, we summarized our recent research on the creation and characterization of nanocomposites synthesized into stimuli-responsible polymers and some advantages and possible disadvantages for their use in chemotherapy and photodynamic antitumor therapy.

N. Kutsevol (✉) · A. Naumenko
Taras Shevchenko National University of Kyiv, Kiev, Ukraine
e-mail: kutsevol@ukr.net

O. Fesenko and L. Yatsenko (eds.), *Nanooptics and Photonics, Nanochemistry and Nanobiotechnology, and Their Applications*, Springer Proceedings in Physics 247, https://doi.org/10.1007/978-3-030-52268-1_10

Table 1 Molecular characteristics of D-*g*-PAA determined by SEC

Sample	$M_w \times 10^{-6}$ (g mol^{-1})	R_g (nm)	M_w/M_n
D-*g*-PAA	2.15	85	1.72

2 Stimuli-Responsive Polymers Nanocarriers

2.1 pH-Sensitive Polymer

The pH-responsive polymers have attracted attention as promising approach for applications in cancer therapy. The normal tissues and blood have pH value of 7.4, but the pH of tumors is from 6.0 to 6.5 [4]. Thus, the use of pH-sensitive nanocarriers can target deliver of the encapsulated antitumor drugs to cancer cells.

A star-like copolymer with dextran (D) core and polyacrylamide (PAA) grafts was used for preparation of pH-sensitive nanocarrier. This polymer was synthesized by grafting PAA chains onto dextran with $M_w = 7 \times 10^4$ g/mol, using a ceric-ion-reduce initiation method [6]. The synthesis, characterization, and analysis of polymer structure were reported in [7]. The theoretical number of grafts for this polymer was equal to 5. Further, this copolymer was referred as D-*g*-PAA. This copolymer was chosen based on our previous research as the most efficient polymer nanocarrier for photodynamic therapy [8].

For transformation of the D-*g*-PAA copolymer in anionic form, the alkaline hydrolysis was used. The anionic polymer was referred as D-*g*-PAA (PE) throughout [7]. The degree of hydrolysis of PAA chains was determined by potentiometric titration and was equal to 43%.

The molecular characteristics of the D-g-PAA copolymer, according to size-exclusion chromatography, are shown in Table 1.

2.2 Thermosensitive Polymer

Poly(*N*-isopropylacrylamide) (PNIPAM) is referred in several reviews as attractive polymer for biomedical application. PNIPAM is soluble in water and has lower critical solution temperature (LCST) close to physiological temperatures [9, 10], that is why drug delivery, biosensors, and bioimaging can be the most promising areas of this polymer application. Below LCST the polymer is soluble, above LCST undergoes a phase transition; then collapse and form aggregates. Linear PNIPAM has an LCST value of approximately 32 °C, its phase transition observes at physiological temperature (37 °C), and therefore, it can be used for controlled release of the drug for cancer therapy [11].

Table 2 Molecular characteristics of D-*g*-PNIPAM determined by SEC

Sample	$M_w \times 10^{-6}$ (g/mol)	M_w/M_n	Dh^{25C} (nm)
D-*g*-PNIPAM	1.03	1.52	40

A star-like copolymer dextran-graft-PNIPAM (D-g-PNIPAM) was referred as efficient nanocarrier for delivery of doxorubicin (Dox) [12]. D-g-PNIPAM is star-like with dextran core and PNIPAM grafts. The conformational transition for this copolymer was registered within the temperature range of 32.6–33.4 °C that was higher than LCST point for linear PNIPAM of similar molecular weight and polydispersity and is closer to physiological temperature (37 °C). A possible tuning of the hydrophobicity of star-like polymer, the regulation of the region of phase transition and size of hydrophobic domains by variation of copolymer internal structure were reported [13]. The number of grafting sites per dextran backbone was equal to 15. The sample was designated as D-*g*-PNIPAM.

The molecular characteristics of D-*g*-PNIPAM copolymer are given in Table 2.

2.3 Preparation of Nanosystems

2.3.1 Reagents

Photosensitizer chlorine e6 (Ce6) from Santa Cruz Biotechnology (USA); doxorubicin hydrochloride (Dox) from Sigma-Aldrich (USA); cisplatin (CPt) from "EBEVE" (Austria); $NaBH_4$; $AgNO_3$; $HAuCl_4$; Hank's balanced salt solution from Sigma-Aldrich (USA); dimethyl sulfoxide (DMSO) from Serva (Germany) were used for nanosystems preparation.

2.3.2 Nanosystem Polymer/AgNPs/CPt

Silver nanoparticles (AgNPs) were synthesized in situ in polymer solution of $AgNO_3$. 2 mL of $AgNO_3$ aqueous solution ($C = 0.1$ M) was added to 5 mL of aqueous solution of polymer ($C = 1 \times 10^{-3}$ g/mL) and stirred for 20 min. Then, 2 mL of aqueous solution of $NaBH_4$ ($C = 0.1$ M) was added and stirred for 30 min. The color of solution turned reddish brown that indicated the formation of AgNPs. 1 mL of *C*Pt ($C = 0.5$ mg/mL) was added to the 1 mL of prepared solution of D-*g*-PAA/AgNPs under stirring for 30 min. A basic solution of nanocomposite containing polymer/AgNPs/CPt was diluted by water to achieve needed concentration of CPt for cytotoxicity experiments.

2.3.3 Nanosystem Polymer/AuNPs

For in situ AuNPs synthesis into polymer solution, tetrachloroauric acid and $NaBH_4$ (reductant) were used. The synthesis process was reported in [14].

2.3.4 Nanosystem Polymer/AuNPs/Ce6/Dox

Ce6 was dissolved in DMSO ($C = 0.182$ mg/mL). Then, 0.55 mL of Ce6 solution was added to 0.27 mL of distilled water. This mixture was added to 1.15 mL of polymer/AuNPs nanosystem, and then, Dox was added. The concentration of Dox in nanocomposite was equal to 0.20 m kg/mL.

2.4 Methods

2.4.1 Fourier Transform Infrared (FTIR) Spectroscopy

Nicolet NEXUS-475 (USA) spectrophotometer was used to obtain FTIR spectra in the range 4000–400 cm^{-1}. The thin films ($l = 6$–9 μm) were fabricated from aqueous solutions of polymer and solution of polymer with addition of CPt or Dox.

2.4.2 Transmission Electron Microscopy (TEM)

The analysis of the nanoparticles was carried on two TEMs, Tecnai G2 or CM12 (FEI, Eindhoven, Netherlands). The images were acquired with a ssCCD Eagle camera on the Tecnai and a Megaview SIS camera. 400 mesh Cu grids with plain carbon film were used for samples preparation (Elmo, Cordouan Technologies, Bordeaux, France).

2.4.3 Quasi-Elastic Light Scattering and Determination of Zeta Potential

Size distribution of scattering objects and zeta potential for nanosystems were performed by quasi-elastic light scattering (QELS) on a Zetasizer Nano-ZS90 (Malvern, Worcestershire, UK) at $T = 298$ K. The instrument was equipped with a He–Ne laser (5 mW) operating at the wavelength of 633 nm. The autocorrelation function of the scattered light intensity was analyzed.

2.5 Biological Examination

2.5.1 Cell Culture

Cell lines were obtained from culture collection of Institute of Molecular Biology and Genetics of NASU (J-774 (murine macrophage cell line), K-562 (human chronic myelogenous leukemia cell line), and U-937 (human histiocytic lymphoma cell line)). All cell lines were maintained in Dulbecco's modified Eagle medium (DMEM) containing 4.00 mM L-glutamine, 4500 mg/mL glucose, and sodium pyruvate. 10% fetal bovine serum (GE Healthcare) and 1% penicillin/streptomycin were added to the culture medium. The cells were cultured in a humidified atmosphere at 37 °C and 5%.

R. E. Kavetsky Institute for Experimental Pathology, Oncology, and Radiobiology NASU provided the MT-4 cells (human T cell leukemia) from The Bank of Cell Lines from human and animal tissue. Cells were maintained in RPMI-1640 containing 10% FBS at 37 °C in humidified atmosphere and 5% CO_2.

Sublines of breast carcinoma MCF-7 cells, namely MCF-7/S—sensitive to cytostatics; MCF-7/Dox—resistant to doxorubicin (Dox), were obtained from the culture bank of the same Institute. Cells were maintained in RPMI-1640 medium containing 10% fetal bovine serum at 37 °C in 95% air and 5% carbon dioxide (CO_2).

2.5.2 In Vitro Study of Nanosystems Cell Viability

MTT assay was used to determine cell viability. Cells were seeded at cell density of 1–105 cells/mL, 100 μL in each of 96 wells. The incubation period was 16 h. Various concentrations of the nanoparticles were used. 10 μL of MTT reagent was added to each well after 48 h incubation and incubated for 4 h. The optical density was measured at 570 nm for the control.

2.5.3 Photodynamic Activity Test

Cell suspensions were prepared from a culture of the malignant cell lines in a log phase of growth. For the preparation, the Hank's balanced salt solution was used. The 1.5-h incubation period for cells in nanocomposite ($t = 37$ °C) was used. After that, the cells were washed twice with fresh Hank's solution. The prepared samples were irradiated with red laser excitation ($\lambda = 658$ nm, power density $= 1.1$ mW/cm^2, dose $= 1$ J/cm^2). After irradiation, the cells were replaced to growth medium, incubated for 18 h ($t = 37$ °C) to finished apoptosis process. The trypan blue dye exclusion test was used to estimate the viability of cells. MTT test was used to determine of the evaluation of dark cytotoxicity of nanocomposites.

3 Results and Discussion

As it was mentioned above, the goal of modern cancer treatment is to kill cancer cells effectively, leaving healthy cells intact. Our research revealed the efficiency of anticancer nanosystems combined the branched copolymer dextran-graft-polyacrylamide and cisplatin. The further attempt was made to improve this nanosytem by adding of silver nanoparticles to nanocomposite.

It was reported that the pH-sensitive copolymer nanocontainers D-g-PAA(PE) was absorbed by macrophages (J-774) and was not cytotoxic [15]. Polymer nanocontainers were completed with the cisplatin-cytotoxic chemotherapy drugs. Complexes of copolymer D-g-PAA(PE)/CPt were synthesized. The FTIR spectra confirmed the complex formation. The FTIR spectra of individual polymer and D-g-PAA(PE)/CPt are represented in Fig. 1.

A nanocomposite polymer/AgNPs and triple nanocomposite polymer/AgNPs/CPt were prepared. The TEM image of these nanosystems is shown in Fig. 2.

Figure 2a demonstrates the presence of nanoparticles with two sizes: 10–15 nm and 2–5 nm due to the interaction of silver ions with carbamide (as in nonionic polymers) and carboxylate groups of the anionic polymer matrix. From Fig. 2b, one can see the partial decreasing of polymer solubility in ternary system polymer/AgNPs/CPt due to complex formation between functional groups of polymer matrix and CPt.

The cytotoxic effects of these nanosystems were tested (Fig. 3).

As it was reported in [16] the results of MTT assays revealed a dose-dependent decrease in viability for both cell lines exposed to either silver- or cisplatin-conjugated nanoparticles. In the study, as anticipated, copolymers did not exhibit any toxicity to both cell types. At the same time, the polymer nanoparticles loaded with cisplatin caused the cytotoxic effect in cell lines at 10 μg/mL (40–44% in U-937),

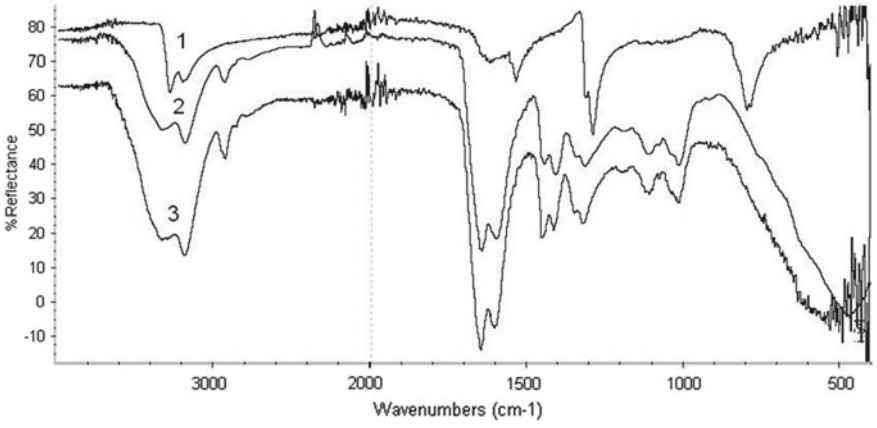

Fig. 1 FTIR spectra for CPt (1), D-*g*-PAA(PE) (2), and D-g-PAA(PE)/CPt (3)

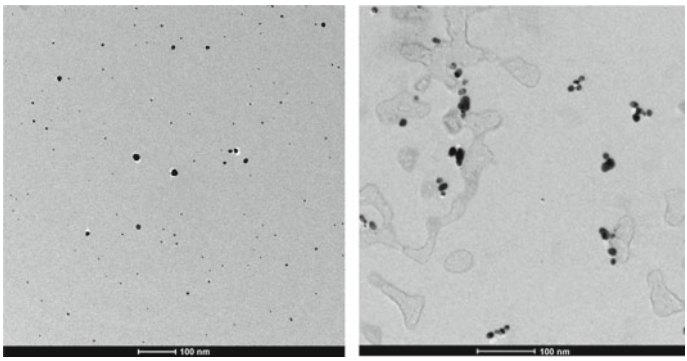

Fig. 2 TEM images of nanosystems polymer/AgNPs (**a**) and polymer/AgNPs/CPt (**b**)

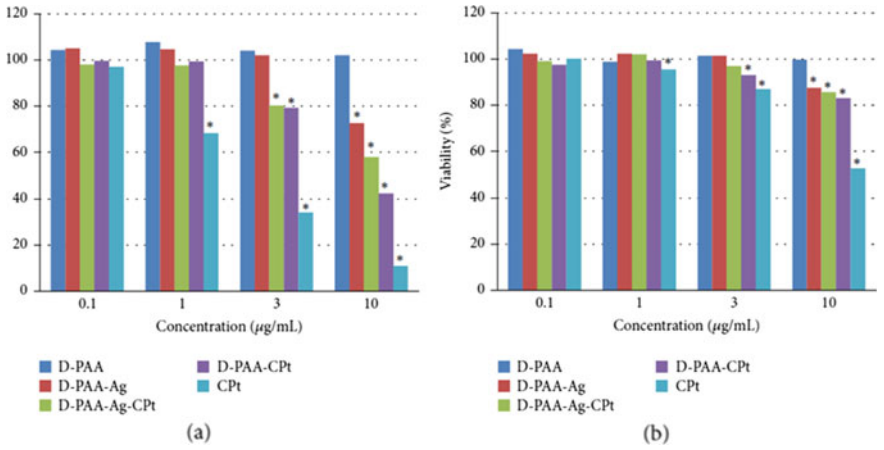

Fig. 3 Viability of the U-937 cells (**a**) and K-562 cells (**b**) after cultivation with the nanoparticles at different concentration for 48 h measured by MTT assay. Mean values of triplicates with standard derivation are shown. $^*P < 0.05$ compared to the untreated control

and so did silver nanoparticles (polymer/AgNPs) at the same concentration (72–76% in U-937 and 86–92% in K-562 provided by MTT assay), although the toxic effect of nanosilver on a cell viability was greater than ones of polymer/cisplatin. Figure 3 demonstrates that a nanosystem where the copolymers were conjugated to both nanosilver and cisplatin displayed less cytotoxic effect compared to the conjugates of dextran-polyacrylamide and cisplatin. It can be deal with some aggregation process which takes place in the ternary nanosystem polymer/AgNPs/CPt (Fig. 2).

A modern trend in photodynamic therapy (PDT) is to use the multifunctional polymer nanocarrier for enhancing target-oriented PDT. The goal of this study was to create hybrid nanocarriers based on the stimuli responsible branched copolymers

D-*g*-PAA(PE) and dextran-*g*-PNIPAM and incorporated AuNPs and photosensitizer, also to try combine PDT with chemotherapy by adding Dox to polymer/AuNPs/Ce6 nanosystem. MT-4 cells were used for testing the ability of these nanosystems onto photodynamic damage. It is very important to estimate the effectiveness of the interaction of the dye molecule with the nanocarrier in nanocomposite photosensitizers (NCPS). That is why we studied how the mass ratio of tetrachloroauric acid to sodium borohydride, which was used as a reducing agent in the synthesis of AuNPs, affects the resulting photodynamic activity of polymer/AuNPs/Ce6 NCPS. The mass ratio of Ce6:AuNPs in all tested samples was 1:10. And the concentration of Ce6 in all samples was equal to 0.1 μg/ml. Figure 4 demonstrates that AuNPs nanocomposite obtained when mass ratio of $HAuCl_4$:$NaBH_4$ during synthesis was 1:2 showed higher photodynamic activity, than Ce6 itself. Nanoparticles synthesis under increase of $NaBH_4$ concentration during the process doesn't affect photodynamic efficacy of nanosystems D-*g*-PNIPAM/AuNPs/Ce6 in comparison with free photosensitizer. However, nanocomposite D-*g*-PAA(PE)/AuNPs/Ce6 ($HAuCl_4$:$NaBH_4$ mass ratio 1:2) demonstrated high enhancement of photodynamic activity in comparison with Ce6 itself.

Namely, this composite has been chosen for preparation of the nanosystem with Dox to combine PDT and chemotherapy. The nanosystems were tested in vitro for its PDT efficiency on the malignant MCF-7/S and MCF-7/Dox cell lines (Fig. 5). The laser irradiation of polymer/AuNPs/Ce6 nanosystem caused the death of 68.4% MCF-7/S cells (Fig. 5a). For MCF-7/Dox cells, nanosystem caused the death of 24.9% (Fig. 5b). However, the activity of nanocomposites containing polymer/AuNPs/Ce6 and Dox for both cell lines was much less.

To understand this phenomenon the three-component nanosystem polymer/AuNPs/Ce6 and four-component nanosystem polymer/AuNPs/Ce6/Dox were studied by DLS at 37 °C. For correct analysis of processes occurring in

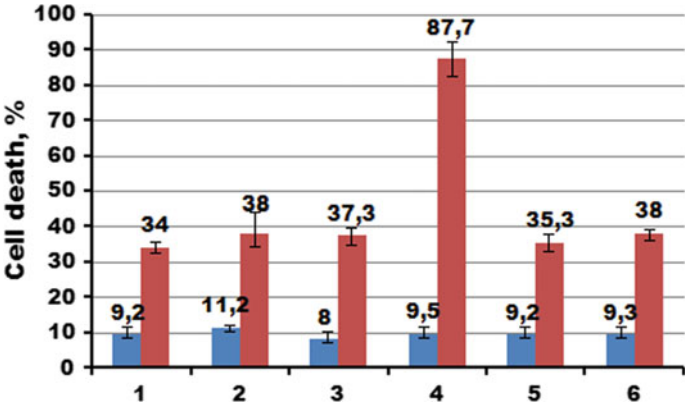

Fig. 4 Dark cytotoxicity and photodynamic activity of polymer/AuNPs/Ce6 nanosystems with different HAuCl4: $NaBH_4$ mass ratios during their synthesis. 1—Ce6 alone; 2—D-*g*-PNIPAM (1:2); 3—D-*g*-PNIPAM (1:4); 4—D-*g*-PAA(PE) (1: 2); 5—D-*g*-PAA(PE) (1:4); 6—D-*g*-PAA(PE) (1: 6)

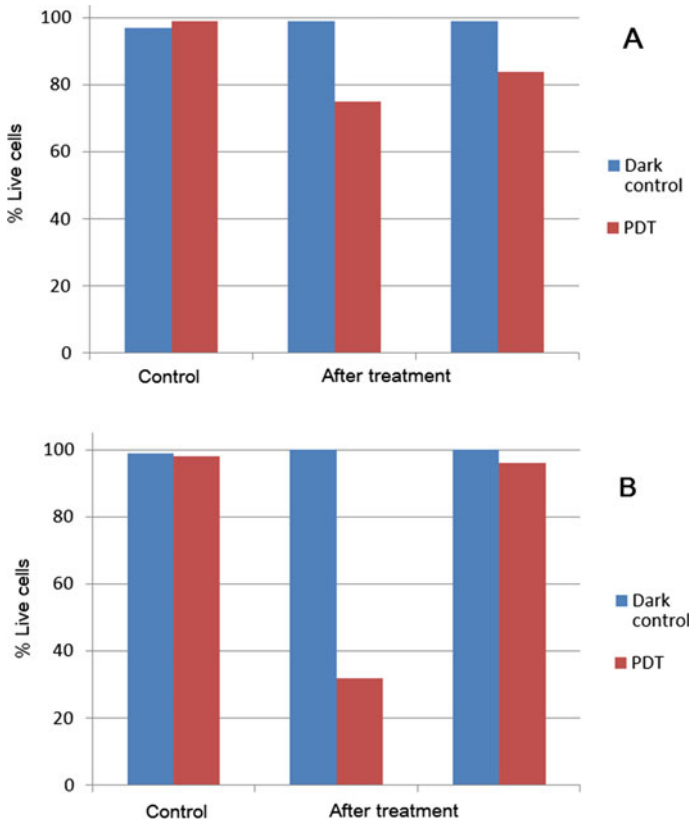

Fig. 5 Effect of PDT on survival of cells—MCF-7/S (**a**), MCF-7/Dox and MCF-7/Ce6 (**b**) lines after the influence of nanocomposites. Control—the same treatment of cells without nanocomposites

multicomponent nanosystems, the author's program for data treatment was used [13]. The size distributions of scattering nanoobjects are shown in Fig. 6.

For three-component nanosystems polymer/AuNPs/Ce6 at 37 °C (Fig. 6, black curve), DLS has revealed several types of scattering nanoobjects. The first maximum corresponds to AgNPs of 10 nm in size. The second maximum can be attributed to the individual macromolecules of 70–80 nm in size with incorporated AgNPs. The third maximum deals with the presence of aggregates of macromolecules of 200–500 nm in size. For four-component nanosystems polymer/AuNPs/Ce6/Dox (Fig. 6, blue curve), AuNPs of 10 nm in size, individual macromolecules, and large aggregates of 800 nm are observed. Obviously, the increased aggregation ability in this nanosystem compared to ones described above is the result of an increase in the number of components included into the macromolecule of the polymer. That leads to change in the hydrophobic-hydrophilic balance of the macromolecule. The strong aggregation process is evident in the TEM images of studied multicomponent nanosystems (Fig. 7).

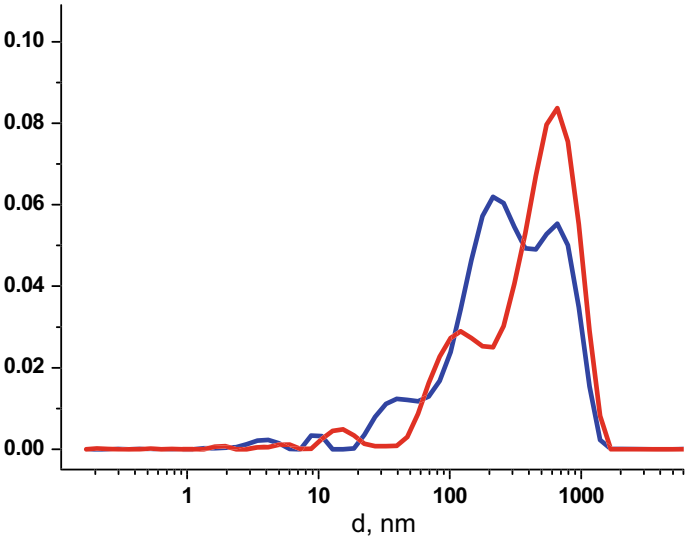

Fig. 6 The dependence of normalized intensity of scattering on hydrodynamic diameter of scattering objects for nanosystems polymer/AuNPs/Ce6 (blue), polymer/AuNPs (red) at 37 °C

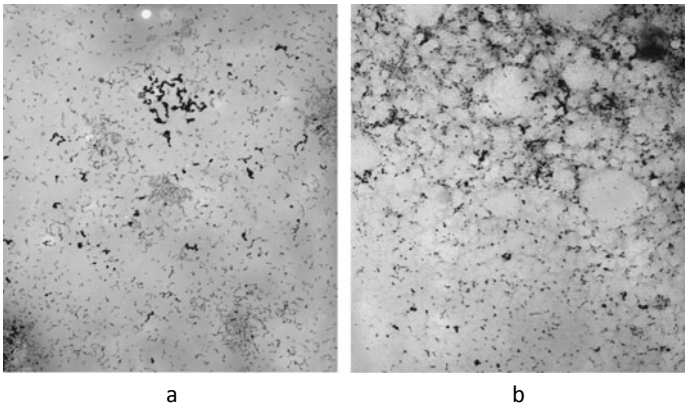

Fig. 7 TEM images of nanosystems: **a** D-*g*-PAA(PE)/AuNPs/Ce6; **b** D-*g*-PAA(PE)/AuNPs/Ce6/Dox

4 Conclusion

Thus, the decreasing of antitumor efficiency of hybrid multicomponent nanosystem synthesized in smart stimuli responsible polymer nanocarriers was registered due to an aggregation process caused by complex formation between functional groups of polymer matrix and encapsulated drugs. As a result, the partial decreasing of polymer

solubility was observed. Thus, we have demonstrated the advantages and possible disadvantages to use the multicomponent nanosystems for antitumor therapy.

Acknowledgements Authors are very grateful to academician V. F. Chekhun—the Director of R. E. Kavetsky Institute for Experimental Pathology, Oncology, and Radiobiology of the National Academy of Sciences of Ukraine, for fruitful collaboration.

References

1. Ganta S, Devalapally H, Shahiwala A, Amiji MJ (2008) A review of stimuli-responsive nanocarriers for drug and gene delivery. Control Releas 126(3):187–204
2. Taghizadeh B, Taranejoo S, Monemian SA, Salehi Moghaddam Z, Daliri K, Derakhshankhah H, Derakhshani Z (2015) Classification of stimuli-responsive polymers as anticancer drug delivery systems. Drug Deliv 22(2):145–155
3. Hatakeyama H (2017) Recent advances in endogenous and exogenous stimuli-responsive nanocarriers for drug delivery and therapeutics. Chem Pharm Bull (Tokyo) 65(7):612–617
4. Vijayakameswara Rao N et al (2018) Recent progress and advances in stimuli-responsive polymers for cancer therapy. Front Bioeng Biotechnol 6:110
5. Gil ES, Hudson SM (2004) Stimuli-responsive polymers and their bioconjugates. Prog Polym Sci 29:1173–1222
6. Bezuglyi M, Kutsevol N, Rawiso M, Bezugla T (2012) Water-soluble branched copolymers dextran-polyacrylamide and their anionic derivates as matrices for metal nanoparticles in-situ synthesis. Chemik 66(8):862–867
7. Kutsevol N, Bezuglyi M, Rawiso M, Bezugla T (2014) Star-like destran-graft-(polyacrylamide-co-polyacrylic acid) copolymers. Macromol Symp 335:12–16
8. Chumachenko VA, Shton IO, Shishko ED, Kutsevol NV, Marinin AI, Gamaleia NF (2016) Branched copolymers dextran-graft-polyacrylamide as nanocarriers for delivery of gold nanoparticles and photosensitizers to tumor cells. In: Fesenko O, Yatsenko L (eds) Springer proceedings in physics "nanophysics, nanophotonics, surface study, and applications", vol 183, pp 379–390
9. Chen S, Zhonh H, Gu B, Wang Y, Li X, Cheng Z, Zhang L, Yao C (2012) Thermosensitive phase behavior and drug release of in situ N-isopropylacrylamide copolymer. Mater Sci Eng C Mater Biol Appl 32:2199–2204
10. Bischofberger I, Trappe V (2015) New aspects in the phase behavior of poly-N-isopropylacrylamide: systematic temperature dependent shrinking of PNIPAM assemblies well beyond the LCST. Sci Rep 5:15520
11. Guan Y, Zhang Y (2011) PNIPAM microgels for biomedical applications: from dispersed particles to 3D assemblies. Soft Matter 7:6375–6384
12. Matvienko T, Sokolova V, Prylutska S, Harahuts Y, Kutsevol N, Kostjukov V, Evstigneev M, Prylutskyy Y, Epple M, Ritter U (2019) In vitro study of the anticancer activity of various Doxorubicin-containing dispersions. Bioimpacts 9(1):59–70
13. ChumachenkoV, Kutsevol N, HarahutsY, Rawiso M, Marinin A, Bulavin L (2017) Star-like dextran-graft-PNiPAM copolymers. Effect of internal molecular structure on the phase transition. J Mol Liq 235:77–82 (2017)
14. Kutsevol N, Glamazda A, Chumachenko V, Harahuts Y, Stepanian S, Plokhotnichenko A, Karachevtsev A (2018) Behavior of hybrid thermosensitive nanosystem dextran-graft-pnipam/gold nanoparticles: characterization within LCTS. J Nanopart Res 20:236
15. Telegeeva P, Kutsevol N, Filipchenko S, Telegeev G (2017) Dextran-polyacrylamide as nanocarrier for targeted delivery of anticancer drugs into tumor cells. In: Mukbaniany O, Abadie M,

Tatrishvili T (eds) Chemical engineering of polymers production of functional and flexible materials, Part 2, pp 183–195
16. Telegeev G, Kutsevol N, Chumachenko V, Naumenko A, Telegeeva P, Filipchenko S, Harahuts Y (2017) Dextran-polyacrylamide as matrices for creation of anticancer nanocomposite. Int J Polymer Sci Article ID 4929857